Published online 20 June 2012 *Nucleic Acids Research, 2012, Vol. 40, No. 16 7753–7765*
doi:10.1093/nar/gks556

An ectopic CTCF-dependent transcriptional insulator influences the choice of Vβ gene segments for VDJ recombination at TCRβ locus

Sweety Shrimali[1], Surabhi Srivastava[1], Garima Varma[1], Alex Grinberg[2], Karl Pfeifer[2] and Madhulika Srivastava[1,*]

[1]National Institute of Immunology, Aruna Asaf Ali Road, New Delhi 110067, India and [2]Program in Genomics of Differentiation, NICHD, NIH, Bethesda, MD 20892, USA

Received April 2, 2012; Revised May 16, 2012; Accepted May 17, 2012

ABSTRACT

Insulators regulate transcription as they modulate the interactions between enhancers and promoters by organizing the chromatin into distinct domains. To gain better understanding of the nature of chromatin domains defined by insulators, we analyzed the ability of an insulator to interfere in VDJ recombination, a process that is critically dependent on long-range interactions between diverse types of *cis*-acting DNA elements. A well-established CTCF-dependent transcriptional insulator, *H19* imprint control region (*H19-ICR*), was inserted in the mouse TCRβ locus by genetic manipulation. Analysis of the mutant mice demonstrated that the insulator retains its CTCF and position-dependent enhancer-blocking potential in this heterologous context *in vivo.* Remarkably, the inserted *H19-ICR* appears to have the ability to modulate *cis*-DNA interactions between recombination signal sequence elements of the TCRβ locus leading to a dramatically altered usage of Vβ segments for Vβ-to-DβJβ recombination in the mutant mice. This reveals a novel ability of CTCF to govern long range *cis*-DNA interactions other than enhancer–promoter interactions and suggests that CTCF-dependent insulators may play a diverse and complex role in genome organization beyond transcriptional control. Our functional analysis of mutated TCRβ locus supports the emerging role of CTCF in governing VDJ recombination.

INTRODUCTION

Insulators prevent interactions between promoters and enhancers in a position-dependent manner due to their ability to influence higher order chromatin structure (1). CTCF (CCCTC-binding factor) appears to be important for their activity as it can facilitate both intrachromosomal and interchromosomal interactions and thus define chromatin domains that may be independently regulated (2). A large number of CTCF binding sites have been identified in mammalian genomes suggesting their extensive involvement in governing *cis*-DNA interactions among regulatory elements (3–5). Whether CTCF defined domains restrict specifically the enhancer–promoter communication relevant for transcriptional regulation or can influence other types of *cis*-DNA interactions in the genome is not currently known.

In this context, antigen receptor loci like IgH, TCRα/δ and TCRβ that code for the immunoglobulin (Ig) and T-cell receptors (TCR), are particularly interesting. By exhibiting long range interactions between different types of elements, they present a useful framework to explore the role of CTCF in defining independently regulated chromatin domains. Enhancer–promoter interactions are necessary for defining the developmental stage specificity of RAG-mediated VDJ recombination at these loci (6). Additionally, recombination requires physical interaction between recombination signal sequence (RSS) elements associated with the V, D and J segments in a combinatorial manner. These segments are located at large distances from each other on the chromosome and higher order chromatin reorganization, manifested as locus contraction, is necessary to bring them together prior to recombination in a lineage specific manner (7,8).

*To whom correspondence should be addressed. Tel: +91 11 26703782; Fax: +91 11 26717104; Email: madhus@nii.res.in

The authors wish it to be known that, in their opinion, the first two authors should be regarded as joint First Authors.

Recent analysis of the IgH and Igκ loci demonstrates that interactions between CTCF binding sites indeed organize the higher order chromatin structure relevant for regulation of transcription and recombination. Multiple CTCF binding sites at these loci were postulated to organize the chromatin in concert with cohesin, Pax5, YY1 etc. (9,10). As predicted, some of the sites are important for enhancer blocking at the IgH locus (11,12). An additional role of CTCF and cohesin in locus contraction seems evident by the multiple interactions between the distantly placed CTCF binding sites at the IgH locus in Pro-B cells (12,13). Knockdown of CTCF led to a partial reduction in these long range interactions thereby supporting the role of CTCF in higher order chromatin organization (14). A conditional knockdown of CTCF in ProB cells demonstrated that CTCF may not be necessary for VDJ recombination *per se* but plays an important role in restricting Igκ enhancer activity and thus influences recombination at this locus (15). While these studies underscore the importance of CTCF for appropriate chromatin organization relevant to VDJ recombination, the manner by which CTCF may impact this process needs further elucidation (16).

To gain further insights into the nature of chromatin domains organized by CTCF and their control on nuclear processes like transcription and VDJ recombination, we adopted a 'gain-of-function' genetic approach. A CTCF binding element [*H19* imprint control region (*H19-ICR*) of the *Igf2*/*H19* locus] was inserted to the murine TCRβ locus by genetic manipulation. We present evidence to show that introduction of ectopic CTCF binding sites from an unrelated locus is sufficient to drastically alter the transcription and recombination patterns at the TCRβ locus.

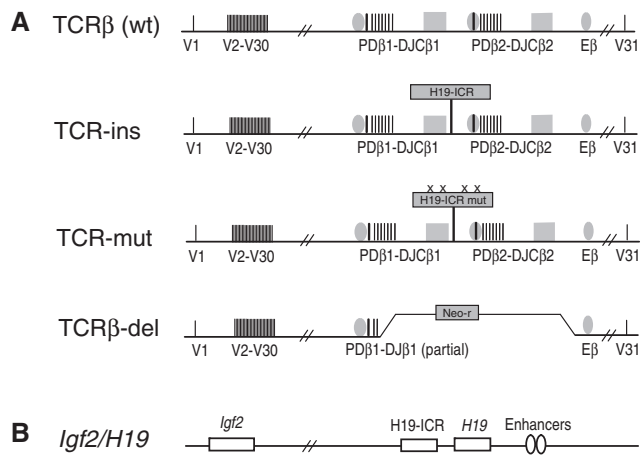

Figure 1. Schematic diagrams showing organization of the genetic loci used for analysis. (**A**) Murine TCRβ loci: wild-type TCRβ locus, mutant TCR-ins locus showing insertion of *H19-ICR*, mutant TCR-mut locus showing insertion of *H19-ICR*-mut with all four CTCF binding sites lost and mutant TCRβ-del locus showing replacement of region encompassing Jβ1.3 to Cβ2 with *neomycin resistance gene* (Neo-r). Grey ovals represent regulatory regions Eβ, PDβ1 and PDβ2 (including 5′PDβ2 and 3′PDβ2 with respect to Dβ2). Each DJCβ cluster has a single Dβ segment (dark vertical line), seven Jβ segments (light vertical lines) and a Cβ region (grey rectangle). The 31 Vβ segments (TRBV1 to TRBV31) are represented as vertical lines (V1 to V31). RSS elements (not shown) are located downstream to each TRBV segment, upstream and downstream to each Dβ segment and upstream to each Jβ segment. (**B**) Murine *Igf2*/*H19* locus showing the endogenous location of *H19-ICR* relative to *Igf2* and *H19* genes and their shared endodermal enhancers. The TCRβ and *Igf2*/*H19* loci span about 700 and 100 kb, respectively, in the mouse genome.

Organization and regulation of murine TCRβ locus, encoding β chain of α/β T cell receptor (α/β TCR), is useful to delineate the interactions of diverse elements. Unlike the relatively large IgH and Igκ loci, TCRβ locus spans only about 700 kb in the genome. It has 31 Vβ gene segments (TRBV1 to TRBV31). Majority of the Vβ segments are located upstream to the two clusters of Dβ and Jβ segments, i.e. Dβ1-Jβ1.1-1.7-Cβ1 (DJCβ1) and Dβ2-Jβ2.1-2.7-Cβ2 (DJCβ2) while the TRBV31 is located downstream to the DJCβ regions (Figure 1A) (17). A developmentally regulated enhancer (Eβ) and promoters PDβ1 and PDβ2 are the key regulatory elements that interact functionally during early double negative (DN, $CD8^-$ $CD4^-$) stage of T cell development (18–21). Their interaction, achieved by formation of a holocomplex comprising enhancer Eβ and promoter PDβ1 and/or PDβ2, leads to generation of chromatin accessibility restricted to about 25 kb region encompassing the DJCβ1 and DJCβ2 clusters (22,23). Consequently, PDβ1 and PDβ2 initiate germline transcripts from DJCβ1 and DJCβ2 clusters, respectively. The altered chromatin also becomes accessible to RAG proteins that orchestrate the RSS-mediated Dβ-to-Jβ recombination at the DJCβ clusters in accordance with the accessibility hypothesis (24). The alleles that have undergone successful Dβ-to-Jβ recombination, act as substrates for RSS-mediated Vβ-to-DβJβ recombination that generates the functional TCRβ gene. Chromatin structure of Vβ segments is also altered in DN T cells but is independent of regulation by Eβ (25). Juxtapositioning of RSS elements associated with Vβ and DβJβ segments is achieved by locus contraction prior to recombination (8). Keeping these observations in mind, we argued that the insertion of a CTCF-dependent insulator at the TCRβ locus could potentially interfere with different aspects of VDJ recombination that may be regulated by Eβ and/or be otherwise influenced by chromatin organization.

We exploited the CTCF-binding activity of the *H19-ICR* of the murine *Igf2*/*H19* locus (Figure 1B) for interfering with TCRβ locus regulation. *H19-ICR* regulates the parent-of-origin specific monoallelic expression of *H19* and *Igf2 in vivo* (26–28). It binds CTCF and organizes an insulator that prevents *Igf2* promoter activation by the downstream enhancers on the maternally inherited allele. Loss of CTCF binding due to methylation of CpG residues prevents binding of CTCF and abrogates enhancer blocking on the paternally inherited allele leading to activation of *Igf2* promoter by the enhancers (29,30). Loss of CTCF binding due to targeted mutations of CTCF binding sites on the maternal allele activates maternal *Igf2* gene emphasizing the crucial link between enhancer blocking and CTCF (31). We chose *H19-ICR* as the insulator to perturb the TCRβ locus because the enhancer blocking by *H19-ICR* is clearly dependent on CTCF. Also, when inserted at the *Afp* locus in mice, *H19-ICR* was able to interact with enhancer and

promoter as it does at the endogenous *Igf2/H19* locus (32). Although the organization of the regulatory elements at the *Afp* locus precluded an unambiguous functional readout of enhancer blocking, these observations suggested that the *H19-ICR* was likely to function as an enhancer blocker in a heterologous context *in vivo*.

Our analysis demonstrates that the inserted *H19-ICR* is capable of curtailing functional enhancer–promoter interaction required not only for transcriptional activation but also for Dβ-to-Jβ recombination in the heterologous context of TCRβ.

Most intriguingly, we find that the usage of Vβ gene segments in the TCRβ chains of the mutant mice is altered. This indicates that the inserted *H19-ICR* can perturb not only enhancer–promoter interactions but can also reorganize the chromatin to influence Vβ-to-DβJβ recombination. These results demonstrate the ability of a CTCF-dependent transcriptional insulator to influence long range DNA interactions necessary for VDJ recombination and provide useful insights into the multiple roles of CTCF in light of the topological model of interactions of regulatory elements in the genome.

MATERIALS AND METHODS

All experiments using mice were conducted as approved by Institutional Animal Ethics Committee. Sequences of all primers are given in Supplementary Table S1.

Targeting the *H19-ICR* and *H19-ICR-mut* to the TCRβ locus

To generate the TCR-ins (Figure 1A), a targeting vector was constructed (Supplementary Figure S1), that had a 5.7 kb BamHI–HindIII fragment and a 4.7 kb HindIII–BamHI fragment from the TCRβ locus as the 5′ flank and 3′ flank, respectively, which originated from 129S6/SvEvTac gDNA. The 2.4 kb BglII fragment carrying the *H19-ICR* fragment with all four CTCF binding sites and a 'neomycin resistance gene' cassette (Neo-r) were cloned between the flanks along with three Lox P sites in tandem orientation. Additionally, 'diphtheria toxin-A' (DTA) gene was also cloned that served as the negative selection marker. The construct was linearized with NotI and electroporated in R1 embryonic stem (ES) cells derived from mouse strain 129X1/SvJ x 129S1 and the clones were selected for G418 resistance. Genomic DNA from G418 resistant clones was digested with BglII and subjected to Southern hybridizations with the 5′ and 3′ probes. The correctly targeted alleles (Tins) generate 6.4 and 7.5 kb bands upon hybridization with the 5′ and 3′ probes, respectively, compared to the 12.6 kb band of the wild-type allele in each case. The Neo-r cassette was subsequently removed by electroporation with a plasmid pBS185 transiently expressing 'Cre recombinase'. The correct clones (TCR-ins), which had excised Neo-r gene but retained the *H19-ICR*, were screened using a PCR-based strategy that detected the insulator-TCRβ junctions on either end. Further, the TCR-ins clones having excision of Neo-r gene were confirmed by Southern hybridization of BglII digested gDNA. The BglII fragment size, detected by 3′ probe, in the non-excised Tins clones is 7.5 kb and changes to 6.4 kb in Neo-r excised TCR-ins clones. Correctly manipulated TCR-ins ES cells were micro-injected into C57bl/6 blastocysts to derive founder chimeric mice that were bred to derive TCR-ins mutant mice. The germline transmission of the mutation in the mice was confirmed by Southern hybridization and PCR analysis (Supplementary Figure S1).

Exactly similar strategy was used for targeting of *H19-ICR*-mut to generate TCR-mut mice. The *H19-ICR*-mut had all the four CTCF binding sites mutated (31).

Generation of the mouse strain TCR-cas

The congenic mouse strain TCR-cas was generated that carried wild-type TCRβ locus derived from *Mus castaneus castaneus* in a *Mus musculus domesticus* genetic background. The female F1 progeny of *Mus castaneus castaneus* × *Mus musculus domesticus* was backcrossed to *Mus musculus domesticus* males for eight generations to derive this strain. At each generation, the presence of *castaneus* sequences upstream and downstream to TCRβ allele was verified by PCR using oligonucleotide primers DMit274 and D6Nds4.

Flow cytometric analysis

Thymocytes from TCR-ins mutant mice and littermate controls were immunostained with anti-CD4-PE (clone RM4-5) and anti-CD8a-Cy5 (clone 53-6.7) and analyzed on BD-LSR Flow Cytometer. For the Vβ choice analysis, these were additionally stained with anti TRBV31-FITC (clone 14-2) or a cocktail of FITC conjugated anti-Vβ antibodies that included anti-TRBV2 (clone KT4), anti-TRBV4 (clone B21.5), anti-TRBV12.1/12.2 (clone MR9-4), anti-TRBV13.1/13.2 (clone MR5-2), anti-TRBV13.3 (clone 1B3.3) and anti-TRBV19 (clone RR4-7). The anti-Vβ antibodies were from the Mouse Vβ TCR screening panel (BD Bioscience cat no. 557004) but Vβ representation is according to IMGT nomenclature. Total thymocytes immunostained with anti-CD4-PE (clone RM4-5), anti-CD8a-Cy5 (clone 53-6.7) and anti-CD25-FITC (clone 7D4) were used to sort DN2/3 thymocytes ($CD4^-$ $CD8^-$ $CD25^+$) on BD FACS ARIA III. The purity of the sorted population was more than 95%. All antibodies were from BD Biosciences, USA.

Allele specific transcriptional analysis by SNAPSHOT assay

Allele specific expression of germline transcripts was analyzed in thymocyte RNA of 4–5 weeks old RAG deficient mice which had maternally inherited *domesticus* allele (wild-type or TCR-ins) and paternally inherited *castaneus* allele (TCR-cas). Random primers were used for the reverse transcription and gene-specific primers were used to amplify DJβ1, DJβ2, TRBV13.2 and TRBV31. The amplified products were subjected to SNAPSHOT analysis (Snapshot multiplex kit, ABI) that relied on incorporation of fluorescently labelled dideoxynucleotides by single nucleotide primer extension (SNuPE) based on specific nucleotide differences between

domesticus and *castaneus* alleles. Detection of incorporation was by ABI Genetic Analyzer 3130x1. Genomic DNA of TCR-cas, C57Bl/6 and C57Bl/6/TCR-cas (F1) were used as controls to verify incorporation of specific nucleotides by *castaneus* and *domesticus* alleles. The incorporation of dideoxynucleotides by F1 gDNA was used to normalize the values for their incorporation in test amplicons (DJβ1, DJβ2, TRBV13.2 and TRBV31) before calculating allele specific contribution of the *doemsticus* (TCR-ins or wild-type) and *castaneus* alleles to total mRNA.

Transcriptional analysis by quantitative RT-PCR

Thymocytes from 6–8 weeks old TCR-ins, TCR-mut and control mice were used to derive total RNA. The RNA was reverse transcribed using random primers and used for quantitative PCR to detect transcripts for DJβ1, DJβ2, Thy1.2, TRBV13-Dβ-Jβ1.1, TRBV31-Dβ-Jβ1.1, TRBV13-Dβ-Jβ2.7 and TRBV31-Dβ-Jβ2.7 using gene specific primers. The forward TRBV13 primer was designed to detect TRBV13.1, TRBV13.2 and TRBV13.3. SYBR-Green chemistry based Real time PCR analysis on ABI PRISM-7000 Sequence Detection System, ABI, USA was used for the quantitative PCR. The amount of transcripts in mutant mice were calculated normalized to the endogenous reference (Thy1.2) and relative to a calibrator (control mice) using the standard curve method for relative quantification.

Dβ-to-Jβ recombination analysis by PCR

Genomic DNA isolated from thymocytes was subjected to PCR and analyzed for the appearance or disappearance of recombination specific bands as described.

DJCβ usage analysis

RNA from thymocytes was reverse transcribed using random primers followed by PCR amplification using gene specific primers to detect rearranged TCRβ genes having TRBV12 (including TRBV12.1 and TRBV12.2), TRBV13 (including TRBV13.1, TRBV13.2 and TRBV13.3) and TRBV31 and any of the two Cβ (Cβ1 or Cβ2). The amplified products were cloned. Sequence analysis from at least 36 clones of each genotype was carried out and fraction of clones using DJCβ1 or DJCβ2 determined.

RESULTS

Genetic manipulation of the TCRβ locus

We used a 'knock-in' approach to insert the *H19-ICR* at the TCRβ locus in mouse ES cells such that the 2.4 kb *H19-ICR* element, carrying all four CTCF binding sites and known to be sufficient for enhancer blocking *in vitro* (30,33), was introduced immediately downstream to the PDβ1-regulated transcription unit comprising Dβ1-Jβ1.1-1.7-Cβ1 (DJCβ1; Figure 1A). This positioned the *H19-ICR* between the promoter PDβ1 and the enhancer Eβ. PDβ2 dual promoters, responsible for the expression of the second transcription unit Dβ2-Jβ2.1-2.7-Cβ2 (DJCβ2), are located downstream to the *H19-ICR* insertion site. Correctly targeted ES cells (TCR-ins) were used to derive mutant mice that carried the *H19-ICR* inserted at the TCRβ locus. To unambiguously ascertain the importance of CTCF in the *H19-ICR* function in the heterologous context, we also generated mutant mice (TCR-mut) that carried a mutant version of *H19-ICR* (*H19-ICR mut*) wherein all the four CTCF binding sites were mutated (Figure 1A). The four site-specific mutations are known to abrogate CTCF binding by *H19-ICR in vitro* as well as *in vivo* (31). All heterozygous and homozygous mutants were viable, fertile and indistinguishable from the wild-type mice in physical appearance.

H19-ICR functions as an enhancer blocker specifically upon maternal inheritance at the endogenous *Igf2*/*H19* locus. Hence, the transcription and recombination analysis was carried out in an allele specific manner. Thymocytes for the analysis were derived from mutant mice that maternally inherited TCR-ins (M, TCR-ins/TCRβ-del), TCR-mut (Mx, TCR-mut/TCRβ-del) or wild-type TCRβ allele (C, +/TCRβ-del). In each case, the presence of TCRβ-del (Figure 1A), carrying 15 kb deletion (encompassing DJCβ1 and DJCβ2) as the paternal allele, ensured that it would not contribute to any analysis as it could neither generate transcripts in the deleted region nor undergo recombination (34,35). Alternatively, using a congenic mouse strain, TCR-cas (see 'Materials and Methods' section for details), mutant mice were obtained that maternally inherited *domesticus* TCR-ins (M*, TCR-ins/TCR-cas) or *domesticus* wild-type TCRβ allele (C*, +/TCR-cas). In each case, the paternally inherited allele was *castaneus* wild-type TCRβ (TCR-cas). Nucleotide differences between the *domesticus* and *castaneus* alleles afforded allele-specific transcriptional analysis of thymocytes in these mice.

H19-ICR insertion at the TCRβ locus does not arrest overall thymocyte development

Thymocyte development proceeds sequentially *via* double negative (DN, $CD4^-CD8^-$), double positive (DP, $CD4^+CD8^+$) and single positive (SP, $CD4^+CD8^-$ and $CD4^-CD8^+$) stages characterized by the presence of cell surface markers CD4 and CD8. The development beyond DN stage depends on the synthesis of a functional TCRβ chain consequent to successful VDJ recombination of TCRβ locus (35). Since the inserted *H19-ICR* could potentially interfere in the regulation of transcription and/or recombination at TCRβ locus, we first examined the effect of our TCRβ manipulation on overall thymocyte development.

The cellularity of the thymus in TCR-ins (M), TCR-mut (Mx) and control (C) mice as well as their thymocyte developmental profiles were comparable (Figure 2). As described above, the TCRβ-del background allele is not capable of supporting recombination and contributing to T-cell development beyond DN stage (35). Therefore, T-cell development beyond DN stage to generate DP and eventually SP thymocytes in the mutant mice demonstrated the ability of the TCR-ins and TCR-mut

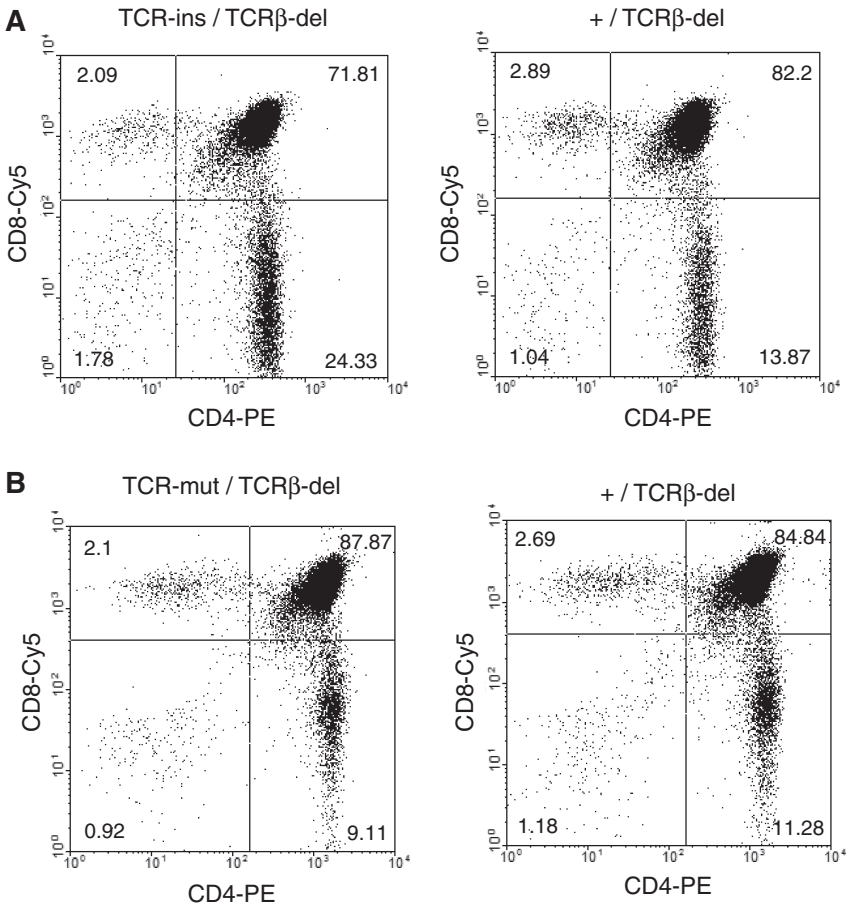

Figure 2. Effect of *H19-ICR* insertion on T-cell development analyzed in thymocytes isolated from mutant mice. (**A**) Mutants that maternally inherited the TCR-ins (TCR-ins/TCRβ-del) or wild-type TCRβ allele (+/TCRβ-del). (**B**) Mutants that maternally inherited TCR-mut (TCR-mut/TCRβ-del) or wild-type TCRβ allele (+/TCRβ-del). Thymocytes were immunostained to detect the presence of cell surface markers CD4 and CD8.

alleles to undergo VDJ recombination and generate functional TCRβ chains. Thus, the inserted *H19-ICR* neither completely abolished VDJ recombination nor arrested thymocyte development. The ability of TCR-ins and TCR-mut mutant alleles to support VDJ recombination cannot be used to simplistically infer that regulation of VDJ recombination was not affected. Multiple Vβ, Dβ and Jβ segments are used in a combinatorial manner during VDJ recombination. Hence, it was plausible that the inserted position-dependent *H19-ICR* insulator influenced transcription and recombination in a gene-segment-specific manner. Thymocytes isolated from the mutant mice were, therefore, utilized to unambiguously investigate gene-segment-specific transcription as well as Dβ-to-Jβ and Vβ-to-DβJβ recombination events at the manipulated alleles.

Effective CTCF-dependent enhancer blocking by inserted *H19-ICR*

We hypothesized that if the *H19-ICR* organized a functional insulator between promoter PDβ1 and enhancer Eβ in the TCR-ins allele, it would reduce the generation of DJβ1 germline transcripts that depend on activation of PDβ1 by Eβ. An assay was designed wherein RT-PCR was followed by SNAPSHOT analysis. Based on this, single nucleotide differences between the *domesticus* and *castaneus* alleles were utilized to determine the contribution of the mutant (TCR-ins) or the wild-type (+) allele to the germline transcripts originating from various promoters of the TCRβ locus in thymocytes of TCR-ins mutants (M*) and control mice (C*). The analysis was performed in RAG deficient mice ($Rag^{-/-}$) to prevent VDJ recombination and avoid heterogeneity in DNA templates that could interfere in accurate detection of germline transcripts.

A drastic reduction in the DJβ1 transcription from the mutant TCR-ins allele was evident as it contributed to less than 5% of the total DJβ1 transcripts in the mutant mice (M*; Figure 3A). The control mice (C*) exhibited nearly equal contribution of the *domesticus* and *castaneus* alleles (biallelic expression) for DJβ1 as expected. We also observed that the expression of DJβ2 transcripts continued to be biallelic in mutants as in the control mice (Figure 3A). Further, the Vβ germline transcripts (TRBV13.2 and TRBV31) also continued to be expressed from both alleles in mutants as in control mice (Figure 3A).

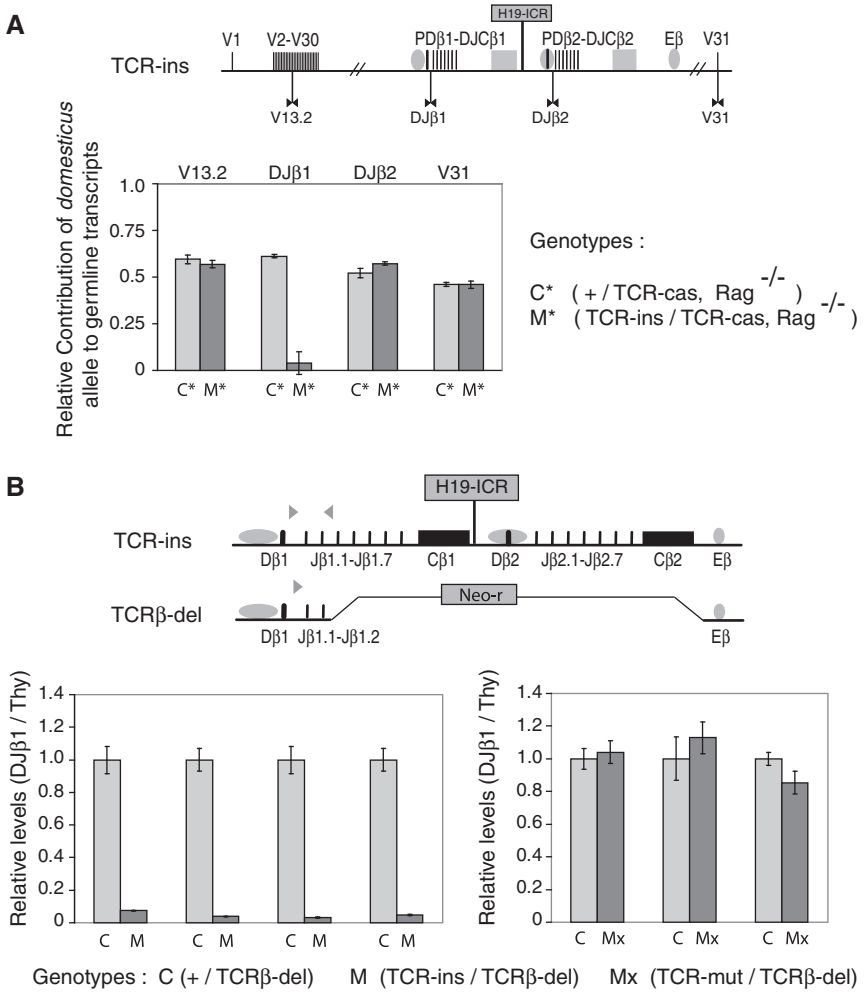

Figure 3. Effect of *H19-ICR* insertion on germline transcription at the TCRβ locus. (**A**) Analysis of allele specific germline transcription initiated by PDβ1, PDβ2 and two Vβ (V13.2 and V31) promoters in RAG deficient TCR-ins mutant mice (M*, TCR-ins/TCR-cas, $Rag^{-/-}$) and control mice (C*, +/TCR-cas, $Rag^{-/-}$) by RT-PCR SNAPSHOT assay. The schematic diagram shows the positions of primers (black triangles) used for PCR amplification. Contribution of *domesticus* allele (TCR-ins or +) calculated as *domesticus*/(*domesticus* + *castaneus*) is plotted. Error bars represent ± SD ($n = 6$). (**B**) Quantitative RT-PCR analysis of Eβ-dependent germline transcripts initiated by PDβ1 promoter in sorted DN2/3 thymocytes of mutants. Schematic diagram shows regulatory regions Eβ, PDβ1 and PDβ2 (grey ovals) and positions of PCR primers (grey triangles) for detecting DJβ1 germline transcripts. Abundance of DJβ1 transcripts was analyzed in thymocytes of mice that were RAG sufficient and inherited TCR-ins maternally (M, TCR-ins/TCRβ-del) or TCR-mut maternally (Mx, TCR-mut/TCRβ-del) relative to control mice (C, +/TCRβ-del), Thy1.2 gene was used as an endogenous control. Error bars depict ± SEM within each experiment ($n = 3$). Each bar denotes RNA analysis of an individual mouse. Analysis done in a single RT-PCR experiment is represented as a group of 2 bars.

The significant impairment in DJβ1 transcripts indicated that the inserted *H19-ICR* abrogates Eβ and PDβ1 interaction necessary for transcriptional activation. Insulators curtail enhancer-based promoter activation only when located between the enhancer and the promoter. Our finding of abrogation of Eβ-PDβ1 interaction taken together with no alteration in Eβ-PDβ2 interaction unambiguously demonstrated that the inserted *H19-ICR* acts as an effective position-dependent enhancer blocking insulator when inserted at the TCRβ locus. The Vβ promoters are known not to be affected by Eβ (25). An unaltered transcriptional profile of Vβ germline transcripts indicated that *H19-ICR* insertion specifically abrogated the Eβ-PDβ1 interaction rather than lead to generalized alterations in germline transcription at the TCRβ locus.

It was important to confirm the abrogation of Eβ-PDβ1 transcription in RAG sufficient ($Rag^{+/+}$) mice since normal RAG expression in the developing T cells was necessary for the analysis of interference of inserted *H19-ICR* with VDJ recombination. To minimize the influence of recombination on detection of germline transcription, DN thymocytes at DN2/3 stage of development were isolated. Such cells have a high proportion of alleles that have not undergone recombination and hence are in the germline configuration. A quantitative RT-PCR assay was designed to specifically estimate the abundance of DJβ1 germline transcripts arising due to Eβ-PDβ1 interaction prior to recombination (Figure 3B). Further, the RT-PCR primer design ensured that the DJβ1 transcripts arising from the paternal TCRβ-del allele were not detected. In this assay also, the DJβ1 transcripts in

mutant mice (M) were observed to be drastically reduced compared to controls (C; Figure 3B, left graph). Further, the Eβ–PDβ2 interaction-dependent DJβ2 germline transcripts continued to be expressed at high levels in TCR-ins mutants (M) like the control mice (C) in the sorted DN2/3 thymocytes (Supplementary Figure S2). It was evident, therefore, that the inserted *H19-ICR* functions as a position-dependent enhancer blocker in RAG sufficient mice also. All subsequent experiments were performed on mice with RAG sufficient background.

Finally, to ascertain the requirement of CTCF for the insulator organized by *H19-ICR*, we analyzed the abundance of DJβ1 germline transcripts in TCR-mut mice (Mx). Clearly, in these mice, the Eβ–PDβ1 interaction-dependent DJβ1 transcription was not affected (Figure 3B, right graph). This demonstrated that the enhancer blocking organized by the inserted *H19-ICR* at the TCRβ locus is CTCF dependent.

Severe abrogation of Eβ–PDβ1 interaction-mediated recombination

Deletion analysis has indicated that the interaction of Eβ with the promoters PDβ1 and PDβ2 leads to generation of chromatin accessibility both for transcription and recombination (22). Since the inserted *H19-ICR* was able to prevent Eβ–PDβ1 interaction-mediated transcriptional activation, we examined its ability to interfere in Dβ-to-Jβ recombination by PCR based on genomic DNA from thymocytes (Figure 4A).

Amplification products of 450 and 318 bp arising due to the recombination of Dβ1 with Jβ1.1 and Jβ1.2, respectively, were evident in control mice (C) but were absent in TCR-ins mutants (M). Further, the 1.1 kb band representing the non-rearranged germline configuration was robustly amplified in mutants (Figure 4A, left panels). This indicated a severe abrogation of recombination at the DJCβ1 cluster. The block in recombination was CTCF dependent as TCR-mut mice (Mx) did not exhibit such an abrogation. In accordance with our observation that *H19-ICR* did not influence Eβ–PDβ2 interaction for transcription, the PDβ2-regulated recombination of Dβ2 with Jβ2 was also not significantly altered in TCR-ins mutants. Both mutants (M) and control littermates (C) exhibited the recombination of Dβ2 with Jβ2.1 and Jβ2.2, evidenced by appearance of 411 and 208 bp band and reduction in amplification of 991 bp band (Figure 4A, right panels). These results suggest that enhancer–promoter interaction-dependent recombination can also be curtailed by an insulator in a position-dependent manner.

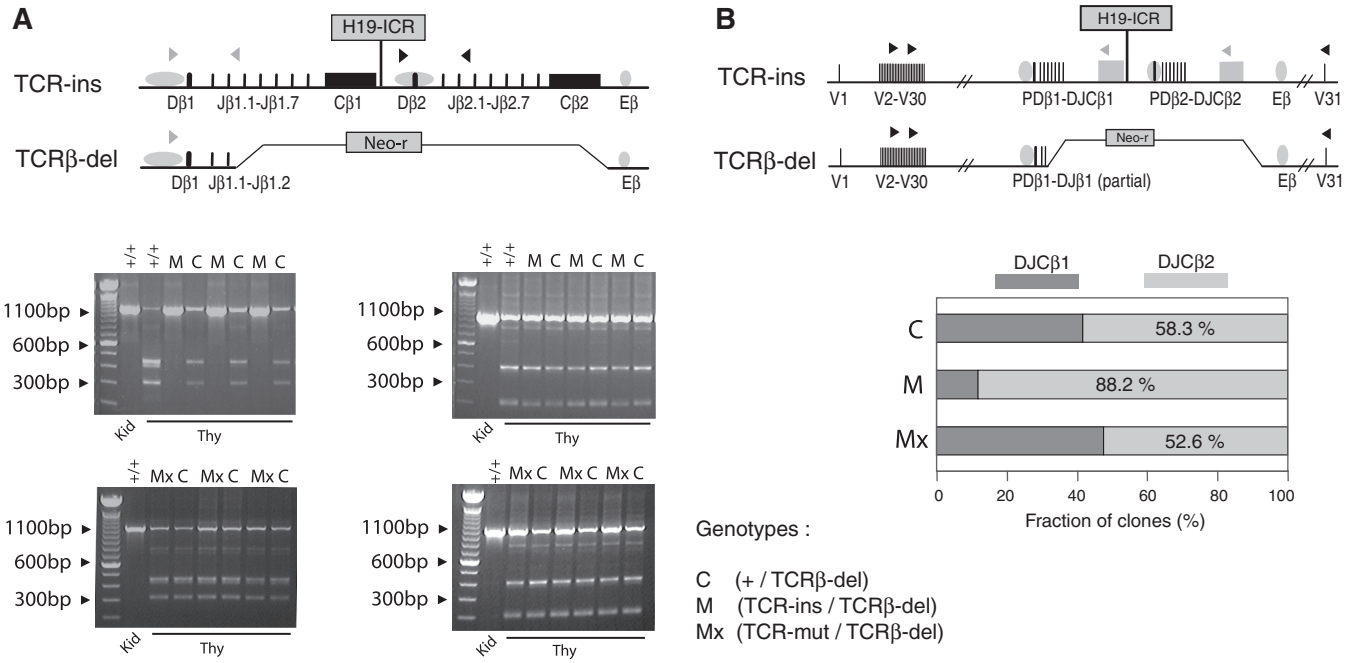

Figure 4. Effect of *H19-ICR* insertion on Dβ-to-Jβ recombination and consequent choice of DJCβ cluster for Vβ-to-DβJβ recombination. (**A**) Recombination at DJCβ1 and DJCβ2 gene clusters. Schematic diagram shows the regulatory regions Eβ, PDβ1 and PDβ2 (grey ovals) and PCR primers (grey and black triangles) that detect Dβ-to-Jβ recombination. Recombination of Dβ1 to Jβ1.1 and Jβ1.2 (left panels) at DJCβ1 and Dβ2 to Jβ2.1 and Jβ2.2 (right panels) at DJCβ2 was analyzed in thymocyte gDNA of TCR-ins mutants (M), TCR-mut mutants (Mx) and control mice (C). Genomic DNA derived from kidney (kid) and thymocytes (Thy) of wild-type mice (+/+) were used as negative and positive controls for Dβ-to-Jβ recombination, respectively. (**B**) Analysis of usage of DJCβ1 and DJCβ2 by the thymocytes for Vβ-to-DβJβ recombination. Schematic diagram shows the positions of primers used for RT-PCR (black and grey arrows) relative to gene segments and regulatory elements of TCRβ locus. Thymocyte RNA was used for RT-PCR using forward primers specific to TRBV12 or TRBV13 or TRBV31 (black arrows on the locus diagram) and a reverse primer common to exon I of both Cβ1 and Cβ2 (grey arrows on the locus diagram). The amplification products were cloned and sequenced to determine the fraction of clones with DJCβ1 or DJCβ2 as depicted in the graph. At least 36 clones were sequenced for each genotype. For PCR and RT-PCR analysis, thymocytes were isolated from mice that maternally inherited the wild-type TCRβ allele (C, +/TCRβ-del) or TCR-ins (M, TCR-ins/TCRβ-del) or TCR-mut (Mx, TCR-mut/TCRβ-del).

Preferential usage of DJCβ2 cluster for VDJ recombination

The TCRβ alleles that have successfully recombined DβJβ regions act as a substrate for RSS-mediated recombination between Vβ and DβJβ segments. The severe reduction in the recombination at DJCβ1 cluster upon maternal inheritance of TCR-ins allele (Figure 4A), was therefore expected to substantially reduce the usage of DJCβ1 region in TCRβ chains in these mutants.

To verify this, RNA was isolated from thymocytes of TCR-ins mutant and control mice. TRBV12 and TRBV13 together contribute to TCRβ chains on about 30% of thymocytes (36). Primers for RT-PCR were designed such that the forward primer could bind to specific Vβ regions (TRBV12, TRBV13 or TRBV31) while the reverse primer was common to exon I of Cβ1 and Cβ2 and avoided any inherent bias for amplification of Cβ1 or Cβ2 (Figure 4B). Amplified products after RT-PCR were cloned and sequenced to estimate the usage of DJCβ1 or DJCβ2 in transcripts encoding TCRβ chain. Sequence analysis revealed a very strong bias in favor of DJCβ2 usage in mice that had maternally inherited TCR-ins (M) and exhibited severely compromised Dβ1-to-Jβ1 recombination compared to the mice that had a wild-type allele (C; Figure 4B). Again, CTCF dependence was clearly evident as the DJCβ2 usage in TCR-mut mice (Mx) was comparable to control mice.

The enhanced usage of DJCβ2 cluster for Vβ-to-DβJβ recombination was a logical consequence of efficient enhancer blocking by the inserted *H19-ICR* that curtailed Eβ-PDβ1 interaction based events, i.e. DJβ1 transcription and Dβ1-to-Jβ1 recombination and hence reduced the usage of DJCβ1 for Vβ-to-DβJβ recombination.

Altered usage of Vβ segments for VDJ recombination

VDJ recombination at TCRβ locus involves long range *cis*-DNA interactions of RSS elements between the recombined DβJβ segments and the Vβ segments located a large distance away. In the TCR-ins allele, in addition to the two DJCβ clusters, Vβ regions also get partitioned by the insulator such that TRBV1-TRBV30 are located upstream to the DJCβ1 cluster and inserted *H19-ICR* while TRBV31 is located downstream to the *H19-ICR* and DJCβ2 cluster (Figure 5A). Having established that the inserted *H19-ICR* organizes a CTCF-dependent functional insulator at TCRβ locus, we analyzed the choice of Vβ gene segments used for Vβ-to-DβJβ recombination in TCR-ins mutant mice.

Thymocytes were analyzed for surface expression of TCRβ that use Vβ gene segments present on either side of the *H19-ICR*. We first analyzed the TRBV31 specific TCRβ by immunostaining thymocytes from TCR-ins mice that organize a functional insulator. We observed an enormous increase (~8- to 10-fold), in the number of CD4-SP thymocytes ($CD4^+CD8^-$) that had TRBV31 in the TCRβ chain in TCR-ins mutants (M; Figure 5B) compared to control littermates (C). Also, in the same thymocyte samples, there was a drastic reduction (about 5-fold) in the usage of several other Vβ tested (TRBV2, TRBV4, TRBV12, TRBV13 and TRBV19). A similarly altered Vβ usage was observed in CD8-SP cells (data not shown). Importantly, such a drastic alteration was not observed for TCR-mut mice (Mx; Figure 5B) that are unable to organize an insulator due to mutated CTCF binding sites.

This suggested that the presence of the ectopic *H19-ICR* insulator is responsible for a decrease in usage of Vβ segments located upstream to the inserted *H19-ICR* and a concomitant increase in the usage of TRBV31 located downstream to the inserted *H19-ICR*. Thus, Vβ choice for Vβ-to-DβJβ recombination was influenced by *H19-ICR* in a CTCF-dependent manner. In conjunction with the increased DJCβ2 usage (Figure 4B), these results suggest a strong bias in favor of TRBV31 recombination specifically with DJCβ2 cluster in the TCR-ins allele. In sharp contrast, recombination of all other Vβ segments with DJCβ2 cluster, i.e. interactions across *H19-ICR*, appear to be hindered significantly.

To confirm our finding, we directly tested the choice of recombination of DJCβ1 and DJCβ2 clusters with TRBV13 and TRBV31. An RT-PCR assay was designed such that the forward primers, in independent PCR reactions, recognize TRBV13 or TRBV31 while the reverse primer recognizes Jβ1.1 in both these reactions. Jβ1.1 was taken as a representative Jβ for the use of DJCβ1 cluster as we observed it to be used maximally in the sequence based analysis of Vβ-to-DβJβ recombination described earlier. In the mice that inherited the TCR-ins maternally (M), there was a drastic reduction in TRBV13-Dβ-Jβ1.1 as well as TRBV31-Dβ-Jβ1.1 transcripts (Figure 6A) consistent with the observation of a reduced ability of DJCβ1 to support Vβ-to-DβJβ recombination (Figure 4A and B).

In a similar assay, by designing the reverse primer in Jβ2.7, we estimated the choice of DJCβ2 for recombination with TRBV13 and TRBV31. In TCR-ins mutants (M), the TRBV31-Dβ-Jβ2.7 transcripts were increased by more than 10-fold while the TRBV13-Dβ-Jβ2.7 transcripts were about 50% less abundant compared to control mice (C; Figure 6B). Thus, effectively, the usage of TRBV31 increased more than 20-fold relative to usage of TRBV13 for recombination to DJCβ2 cluster in the presence of a functional insulator (Figure 6C, upper graph). Unlike TCR-ins mutants (M), TCR-mut mice (Mx) did not exhibit any enhancement in the TRBV31-Dβ-Jβ2.7 to TRBV13-Dβ-Jβ2.7 transcript ratio compared to control mice (C; Figure 6C, lower graph).

Our results indicate that the *H19-ICR* significantly alters the regulation of transcription as well as recombination at the TCRβ locus and this effect is not merely due to the presence of an inserted 2.2 kb DNA fragment. Ability of inserted *H19-ICR* to bind CTCF was essential for its influence on these processes. Just as it prevents the enhancer–promoter communication when present between them, the *H19-ICR* insulator also prevented RSS elements from interacting with each other in a CTCF-and position-dependent manner, i.e. when located between them and led to an alteration in the choice of Vβ segments for recombination (Figure 6D).

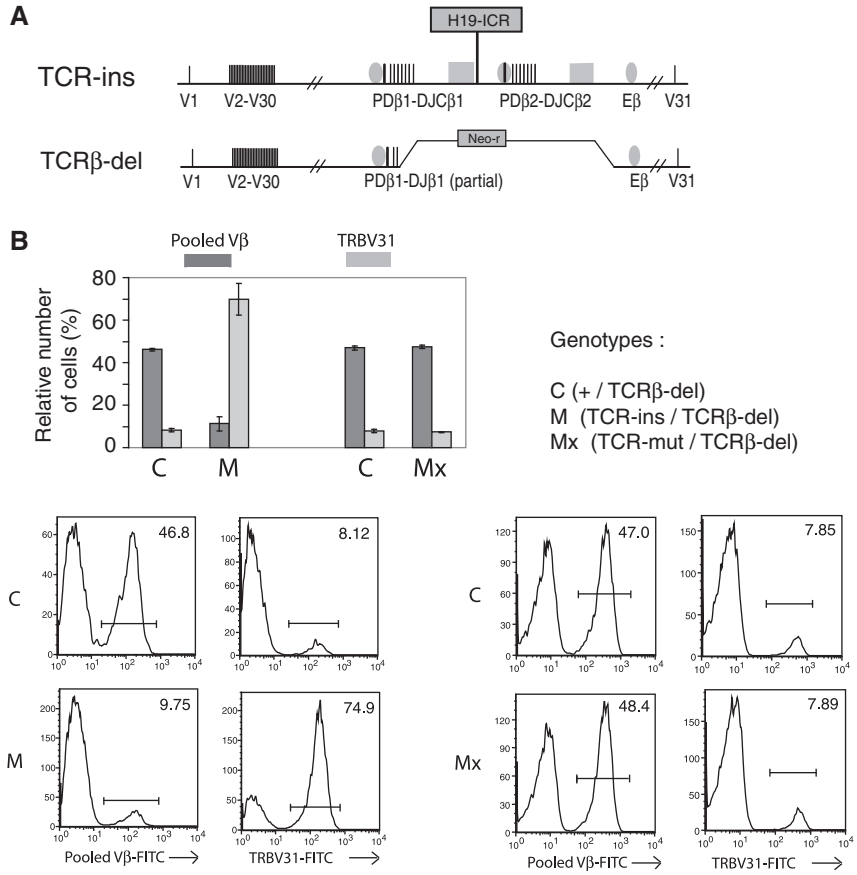

Figure 5. Altered usage of Vβ segments for V to DJ recombination at the TCRβ locus due to *H19-ICR* insertion. (**A**) Schematic diagram of the TCRβ locus showing relevant gene segments and regulatory elements along with the *H19-ICR* insertion. (**B**) Usage of Vβ segments for Vβ-to-DβJβ recombination analyzed by flow cytometry. Thymocytes were immunostained to detect the presence of CD4, CD8 and TRBV31 or CD4, CD8 and pooled Vβ (TRBV2, TRBV4, TRBV12, TRBV13 and TRBV19) on the cell surface. Results from the gated CD4-SP thymocyte population ($CD4^+CD8^-$) are shown in the bar graph as relative numbers of cells that express TRBV31 or any of other Vβ that was included in the pooled Vβ (TRBV2, TRBV4, TRBV12, TRBV13 and TRBV19) in mice that maternally inherited wild-type TCRβ allele (C, +/TCRβ-del) or TCR-ins (M, TCR-ins/TCRβ-del) or TCR-mut (Mx, TCR-mut/TCRβ-del). Error bars represent ± SD between independent experiments ($n = 6$ for M and C and $n = 3$ for Mx and C). Histograms depict representative results from individual FACS experiments as described above. Numbers within the histograms denote the percentage of CD4-SP thymocytes positive for the Vβ under investigation (TRBV31 or pooled Vβ).

DISCUSSION

In this investigation, we took advantage of the precisely regulated transcription and recombination at the TCRβ locus to understand the ability of a CTCF-dependent insulator to interfere in the interactions between several *cis*-acting regulatory elements. By organizing an ectopic insulator at TCRβ locus, we demonstrate a novel ability of CTCF to modulate *cis*-DNA interactions between RSS elements during VDJ recombination.

Our analysis of the TCR-ins and TCR-mut alleles indicated that *H19-ICR* acts as an efficient CTCF-dependent enhancer blocker when inserted to the TCRβ locus and prevents Eβ-regulated transcription and recombination. *H19-ICR* interacts with several CTCF and cohesin binding sites at the *Igf2*/*H19* locus (37) for organizing insulator function. However, it also interacts with enhancer and promoter elements at the *Igf2*/*H19* locus and when inserted at the *Afp* locus suggesting context independence (32). Our analysis confirms the context independence functionally and clearly establishes the ability of the *H19-ICR* to act as a position-dependent enhancer blocker in the absence of any specific *cis*-acting elements of the *Igf2*/*H19* locus *in vivo*.

Effective organization of an insulator by the inserted *H19-ICR* at the TCRβ locus also led to a marked reduction in the Eβ–PDβ1-dependent recombination between Dβ1 and Jβ1 segments. As predicted by the accessibility hypothesis (24), deletion of accessibility control elements (ACE), i.e. either Eβ or PDβ1, has been shown to lead to loss of accessibility generation for transcriptional activation and subsequent recombination (22). Our results provide a strong support for the accessibility hypothesis by relying on a novel approach of altering the ACE activity rather than deletion. Modified histones acetyl-H3K9 and trimethyl-H3K4 have been observed to be associated with chromatin which is accessible for RAG mediated recombination at the antigen receptor loci (38,39). Predictably, an altered epigenetic landscape of TCRβ locus due to the ectopic insulator is the basis for the observed curtailment of Eβ-dependent transcription

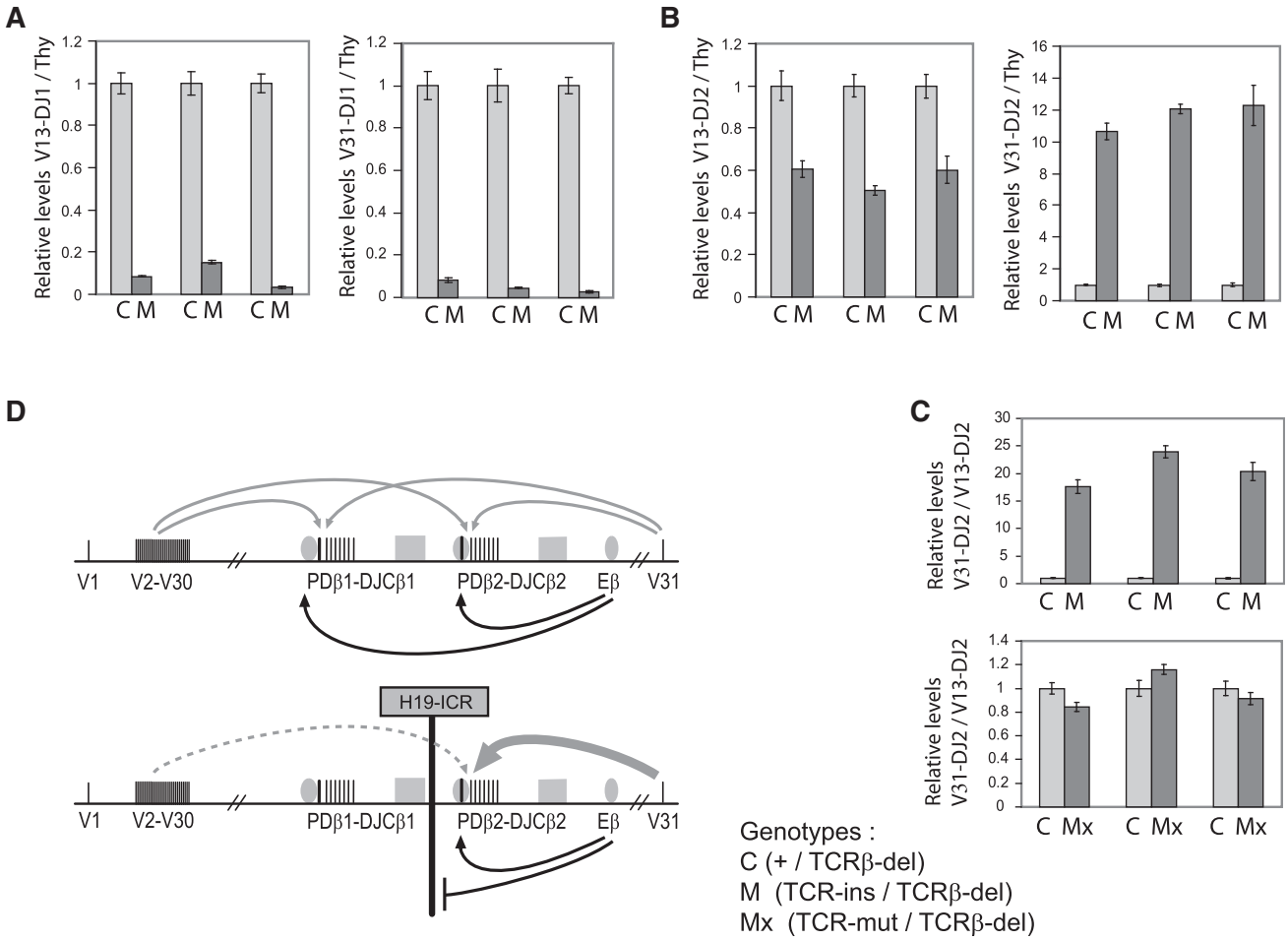

Figure 6. RSS-mediated interactions between chromatin domains defined by *H19-ICR* at TCRβ locus as assessed by relative abundance of transcripts arising due to RSS-mediated recombination in mutants maternally inheriting wild-type TCRβ allele (C, +/TCRb-del), TCR-ins (M, TCR-ins/TCRbdel) or TCR-mut (Mx, TCR-mut/TCRβ-del). (**A**) Abundance of transcripts arising due to recombination TRBV13-Dβ-Jβ1.1 (denoted V13-DJ1) and TRBV31-Dβ-Jβ1.1 (denoted V31-DJ1). (**B**) Abundance of transcripts arising due to recombination TRBV13-Dβ-Jβ2.7 (denoted V13-DJ2) and TRBV31-Dβ-Jβ2.7 (denoted V31-DJ2). (**C**) Abundance of recombined transcripts V31-DJ2 relative to V13-DJ2. In each case, relative abundance was estimated by real-time quantitative RT-PCR analysis. Error bars denote ± SEM. (**D**) Schematic of TCRβ locus in wild-type (upper) and TCR-ins (lower) mice. Arrows indicate the long range interactions necessary for promoter activation (black arrows) and RSS-mediated recombination (grey arrows) between Vβ and DJCβ regions. *H19-ICR* presence in TCR-ins drastically reduces Eβ based PDβ1 activation. It also defines chromatin domains such that 'intradomain' interaction (TRBV31 to DJCβ2 recombination) is significantly increased at the expense of 'interdomain' interaction (TRBV13 to DJCβ2 recombination).

and recombination in TCR-ins mutant alleles. Hence, an extensive comparison of the epigenetic landscape in wild-type TCRβ and TCR-ins alleles is likely to provide useful insights into the nature of ACE interactions and their ability to alter the chromatin accessibility necessary for transcription and RAG-mediated recombination. Further, the promoters PDβ1, 5′PDβ2 and 3′PDβ2 are all regulated by Eβ but exhibit subtle differences in temporal regulation (21). Due to the drastic reduction in Eβ–PDβ1 interaction, the TCR-ins allele provides a useful model to understand the basis for the possible competition between the promoters for the shared enhancer as well as their temporal regulation.

The most remarkable feature that emerged in this study was an alteration in the Vβ usage during VDJ recombination due to introduction of the four ectopic CTCF binding sites. An important role of CTCF in VDJ recombination by defining functional domains was recently demonstrated at IgH and Igκ loci. At these loci, CTCF-defined chromatin loops seem to insulate the proximal V regions from the influence of enhancers Eμ and iEκ. Consequently, the usage of V segments was altered at IgH locus upon deletion of CTCF binding sites (12,40) and at Igκ locus upon loss of CTCF (15) or deletion of the CTCF and Ikaros binding element Sis (41). In the present investigation, we show that the normal chromatin interactions for ordered VDJ recombination can be altered simply by the ectopic insertion of non-locus specific CTCF binding sites. Specifically, we found that TRBV31 usage was drastically enhanced in TCR-ins allele while the usage of Vβ segments located upstream was concomitantly reduced for recombination with DJCβ2. Unlike the V regions of IgH and Igκ, the Vβ segments of TCRβ are not regulated by Eβ (25). Accordingly, the germline transcription of upstream Vβ segment (TRBV13.2) continued to be unaffected by the

insertion of an enhancer blocker. Also, the transcriptional status of TRBV31, located relatively close to Eβ, was not altered in the TCR-ins allele. Yet the Vβ-to-DβJβ recombination profile was completely altered. The most plausible explanation for the altered Vβ usage in TCR-ins allele appears to be the CTCF-directed chromatin domain organization such that the RSS-mediated V-to-DJ recombination is efficient only when V and DJ segments share the same domain defined by CTCF (Figure 6). This suggests that insulators may have the potential to organize specific functional domains with respect to recombination at the antigen receptor loci in addition to their well known ability to define transcriptionally distinct domains. Taken together with the recent evidence from IgH and Igκ loci, these data present an emerging picture of CTCF and insulator elements governing multiple chromatin interactions at the recombining loci.

Chromatin loop organization is mediated by multiple CTCF and cohesin binding sites at the recombining loci (16,42). Based on analysis of IgH locus, it has been proposed that CTCF organizes dynamic rosette structures to facilitate access to all Vh segments for recombining with DhJh segments (43). CTCF manifests its influence by organizing chromatin loops (2). Consequently, the interactions between DNA elements can be promoted as well as hindered depending on their positions relative to the CTCF-binding insulator (2,44). Keeping this in mind, we designed the TCR-ins allele such that the *H19-ICR* insulator effectively partitioned the TCRβ locus. We observed increased intradomain and reduced interdomain functional interactions between promoter–enhancer regulatory elements as well as between RSS elements across the *H19-ICR* insertion in the TCR-ins allele. Thus, CTCF appears to have three activities that impact VDJ recombination: (i) enhancer blocking that regulates ordered assembly of genes (12), (ii) contraction of loci prior to recombination (13,14,16) and (iii) organization of chromatin domains that define the choice of recombining gene segments as observed during this investigation. These activities complement each other and emphasize the importance of CTCF for VDJ recombination. More detailed investigations of the interactions between the ectopic and endogenous CTCF binding sites at the TCRβ locus as well as at other antigen receptor loci will be meaningful to elucidate these roles in future.

Finally, our results also provide useful insights into the nature of interactions between distantly placed *cis*-acting regulatory elements which have, so far, been considered only in the context of transcriptional regulation using chromosome conformation capture (3C) analysis (32,45–47). Enhancers can activate their cognate promoters in a contact-dependent and contact-independent manner according to the topological loop domain and tracking models, respectively. Accordingly, the intervening insulator may either organize the chromatin domains to abrogate enhancer–promoter contact or prevent the tracking signal from reaching the cognate promoter (48). A fundamental assumption of the topological model is that 'intradomain' contacts are favored over 'interdomain' contacts when an insulator defines the distinct domains. This has been difficult to test functionally as reduction in interdomain promoter–enhancer contacts by the intervening insulator cannot be unambiguously discriminated from the block in tracking by an intervening insulator; both the situations would lead to a loss in transcriptional activation.

In this context, it was intriguing to note that the functional *H19-ICR* insulator was able to hinder RSS contact mediated Vβ-to-DβJβ recombination across itself just as it prevents enhancer–promoter functional interaction. VDJ recombination unambiguously relies on a contact based RSS interaction and 'captures' the physical juxtaposition of the interacting RSS elements *in vivo* reporting it as a specific recombination event. When *H19-ICR* defined the chromatin domains at the TCRβ locus, the contact between RSS elements and consequent Vβ-to-DβJβ recombination, was strongly favored between RSS elements sharing the same chromatin domain (intradomain) rather than those separated by the insulator (interdomain; Figure 6D). Mechanistically, RSS-mediated recombination and enhancer-mediated promoter activation are entirely distinct. The only common feature between them is that both require interaction of specific *cis*-acting DNA elements. The ability of the insulator to interfere in a position-dependent manner with each of these distinct processes provides functional evidence to support the topological model of interaction of *cis* acting regulatory elements.

In conclusion, our analysis clearly demonstrates a previously unreported ability of a CTCF-dependent insulator to modulate interactions between RSS elements during VDJ recombination. This emphasizes that the CTCF binding sites may have a complex role in influencing functional interactions between regulatory elements beyond modulating enhancer–promoter interactions and defining transcriptionally independent domains in the genome.

SUPPLEMENTARY DATA

Supplementary Data are available at NAR Online: Supplementary Table 1 and Supplementary Figures 1 and 2.

ACKNOWLEDGEMENTS

We thank Dr. Christopher Schoenherr for providing the plasmid with *H19-ICR*-mut. We also thank Dr. Satyajit Rath and Dr. Ayub Qadri for useful discussions and Ramesh Yadav for technical assistance.

FUNDING

Department of Biotechnology, India (research grants BT/PR3815/BRB/10/318/2003 and BT/PR9088/BRB/10/538/2007 to M.S.); Council of Scientific and Industrial Research, India (Senior Research Fellowship to Sw.S.). National Institute of Immunology (support to Su.S. and M.S.); NICHD Division of Intramural Research (support to A.G. and K.P.). Funding for open access charge: Core Funds of National Intitute of Immunology, New Delhi.

Conflict of interest statement. None declared.

REFERENCES

1. Wallace,J.A. and Felsenfeld,G. (2007) We gather together: insulators and genome organization. *Curr. Opin. Genet. Dev.*, **17**, 400–407.
2. Phillips,J.E. and Corces,V.G. (2009) CTCF: master weaver of the genome. *Cell*, **137**, 1194–1211.
3. Xie,X., Mikkelsen,T.S., Gnirke,A., Lindblad-Toh,K., Kellis,M. and Lander,E.S. (2007) Systematic discovery of regulatory motifs in conserved regions of the human genome, including thousands of CTCF insulator sites. *Proc. Natl Acad. Sci. USA*, **104**, 7145–7150.
4. Kim,T.H., Abdullaev,Z.K., Smith,A.D., Ching,K.A., Loukinov,D.I., Green,R.D., Zhang,M.Q., Lobanenkov,V.V. and Ren,B. (2007) Analysis of the vertebrate insulator protein CTCF-binding sites in the human genome. *Cell*, **128**, 1231–1245.
5. Chen,X., Xu,H., Yuan,P., Fang,F., Huss,M., Vega,V.B., Wong,E., Orlov,Y.L., Zhang,W., Jiang,J. *et al.* (2008) Integration of external signaling pathways with the core transcriptional network in embryonic stem cells. *Cell*, **133**, 1106–1117.
6. Schlissel,M.S. (2003) Regulating antigen-receptor gene assembly. *Nat. Rev. Immunol.*, **3**, 890–899.
7. Roldan,E., Fuxa,M., Chong,W., Martinez,D., Novatchkova,M., Busslinger,M. and Skok,J.A. (2005) Locus 'decontraction' and centromeric recruitment contribute to allelic exclusion of the immunoglobulin heavy-chain gene. *Nat. Immunol.*, **6**, 31–41.
8. Skok,J.A., Gisler,R., Novatchkova,M., Farmer,D., de Laat,W. and Busslinger,M. (2007) Reversible contraction by looping of the Tcra and Tcrb loci in rearranging thymocytes. *Nat. Immunol.*, **8**, 378–387.
9. Degner,S.C., Wong,T.P., Jankevicius,G. and Feeney,A.J. (2009) Cutting edge: developmental stage-specific recruitment of cohesin to CTCF sites throughout immunoglobulin loci during B lymphocyte development. *J. Immunol.*, **182**, 44–48.
10. Ebert,A., McManus,S., Tagoh,H., Medvedovic,J., Salvagiotto,G., Novatchkova,M., Tamir,I., Sommer,A., Jaritz,M. and Busslinger,M. (2011) The distal V(H) gene cluster of the Igh locus contains distinct regulatory elements with Pax5 transcription factor-dependent activity in pro-B cells. *Immunity*, **34**, 175–187.
11. Featherstone,K., Wood,A.L., Bowen,A.J. and Corcoran,A.E. (2010) The mouse immunoglobulin heavy chain V-D intergenic sequence contains insulators that may regulate ordered V(D)J recombination. *J. Biol. Chem.*, **285**, 9327–9338.
12. Guo,C., Yoon,H.S., Franklin,A., Jain,S., Ebert,A., Cheng,H.L., Hansen,E., Despo,O., Bossen,C., Vettermann,C. *et al.* (2011) CTCF-binding elements mediate control of V(D)J recombination. *Nature*, **477**, 424–430.
13. Guo,C., Gerasimova,T., Hao,H., Ivanova,I., Chakraborty,T., Selimyan,R., Oltz,E.M. and Sen,R. (2011) Two forms of loops generate the chromatin conformation of the immunoglobulin heavy-chain gene locus. *Cell*, **147**, 332–343.
14. Degner,S.C., Verma-Gaur,J., Wong,T.P., Bossen,C., Iverson,G.M., Torkamani,A., Vettermann,C., Lin,Y.C., Ju,Z., Schulz,D. *et al.* (2011) CCCTC-binding factor (CTCF) and cohesin influence the genomic architecture of the Igh locus and antisense transcription in pro-B cells. *Proc. Natl Acad. Sci. USA*, **108**, 9566–9571.
15. de Almeida,R.C., Stadhouders,R., de Bruijn,M.J., Bergen,I.M., Thongjuea,S., Lenhard,B., van Ijcken,W., Grosveld,F., Galjart,N., Soler,E. *et al.* (2011) The DNA-binding protein CTCF limits proximal Vkappa recombination and restricts kappa enhancer interactions to the immunoglobulin kappa light chain locus. *Immunity*, **35**, 501–513.
16. Chaumeil,J. and Skok,J.A. (2012) The role of CTCF in regulating V(D)J recombination. *Curr. Opin. Immunol.*, **24**, 153–159.
17. Sikes,M.L. and Oltz,E.M. (2012) Genetic and epigenetic regulation of Tcrb gene assembly. *Curr. Top. Microbiol. Immunol.*, **356**, 91–116.
18. Bouvier,G., Watrin,F., Naspetti,M., Verthuy,C., Naquet,P. and Ferrier,P. (1996) Deletion of the mouse T-cell receptor beta gene enhancer blocks alphabeta T-cell development. *Proc. Natl Acad. Sci. USA*, **93**, 7877–7881.
19. Bories,J.C., Demengeot,J., Davidson,L. and Alt,F.W. (1996) Gene-targeted deletion and replacement mutations of the T-cell receptor beta-chain enhancer: the role of enhancer elements in controlling V(D)J recombination accessibility. *Proc. Natl Acad. Sci. USA*, **93**, 7871–7876.
20. Whitehurst,C.E., Schlissel,M.S. and Chen,J. (2000) Deletion of germline promoter PD beta 1 from the TCR beta locus causes hypermethylation that impairs D beta 1 recombination by multiple mechanisms. *Immunity*, **13**, 703–714.
21. McMillan,R.E. and Sikes,M.L. (2008) Differential activation of dual promoters alters D{beta}2 germline transcription during Thymocyte development. *J. Immunol.*, **180**, 3218–3228.
22. Oestreich,K.J., Cobb,R.M., Pierce,S., Chen,J., Ferrier,P. and Oltz,E.M. (2006) Regulation of TCRbeta gene assembly by a promoter/enhancer holocomplex. *Immunity*, **24**, 381–391.
23. Carabana,J., Watanabe,A., Hao,B. and Krangel,M.S. (2011) A barrier-type insulator forms a boundary between active and inactive chromatin at the murine TCRbeta locus. *J. Immunol.*, **186**, 3556–3562.
24. Sleckman,B.P., Gorman,J.R. and Alt,F.W. (1996) Accessibility control of antigen-receptor variable-region gene assembly: role of cis-acting elements. *Annu. Rev. Immunol.*, **14**, 459–481.
25. Mathieu,N., Hempel,W.M., Spicuglia,S., Verthuy,C. and Ferrier,P. (2000) Chromatin remodeling by the T cell receptor (TCR)-beta gene enhancer during early T cell development: implications for the control of TCR-beta locus recombination. *J. Exp. Med.*, **192**, 625–636.
26. Leighton,P.A., Ingram,R.S., Eggenschwiler,J., Efstratiadis,A. and Tilghman,S.M. (1995) Disruption of imprinting caused by deletion of the H19 gene region in mice. *Nature*, **375**, 34–39.
27. Thorvaldsen,J.L., Duran,K.L. and Bartolomei,M.S. (1998) Deletion of the H19 differentially methylated domain results in loss of imprinted expression of H19 and Igf2. *Genes Dev.*, **12**, 3693–3702.
28. Srivastava,M., Hsieh,S., Grinberg,A., Williams-Simons,L., Huang,S.P. and Pfeifer,K. (2000) H19 and Igf2 monoallelic expression is regulated in two distinct ways by a shared cis acting regulatory region upstream of H19. *Genes Dev.*, **14**, 1186–1195.
29. Bell,A.C. and Felsenfeld,G. (2000) Methylation of a CTCF-dependent boundary controls imprinted expression of the Igf2 gene. *Nature*, **405**, 482–485.
30. Hark,A.T., Schoenherr,C.J., Katz,D.J., Ingram,R.S., Levorse,J.M. and Tilghman,S.M. (2000) CTCF mediates methylation-sensitive enhancer-blocking activity at the H19/Igf2 locus. *Nature*, **405**, 486–489.
31. Schoenherr,C.J., Levorse,J.M. and Tilghman,S.M. (2003) CTCF maintains differential methylation at the Igf2/H19 locus. *Nat. Genet.*, **33**, 66–69.
32. Yoon,Y.S., Jeong,S., Rong,Q., Park,K.Y., Chung,J.H. and Pfeifer,K. (2007) Analysis of the H19ICR insulator. *Mol. Cell Biol.*, **27**, 3499–3510.
33. Kaffer,C.R., Srivastava,M., Park,K.Y., Ives,E., Hsieh,S., Batlle,J., Grinberg,A., Huang,S.P. and Pfeifer,K. (2000) A transcriptional insulator at the imprinted H19/Igf2 locus. *Genes Dev.*, **14**, 1908–1919.
34. Mombaerts,P., Clarke,A.R., Hooper,M.L. and Tonegawa,S. (1991) Creation of a large genomic deletion at the T-cell antigen receptor beta-subunit locus in mouse embryonic stem cells by gene targeting. *Proc. Natl Acad. Sci. USA*, **88**, 3084–3087.
35. Mombaerts,P., Clarke,A.R., Rudnicki,M.A., Iacomini,J., Itohara,S., Lafaille,J.J., Wang,L., Ichikawa,Y., Jaenisch,R., Hooper,M.L. *et al.* (1992) Mutations in T-cell antigen receptor genes alpha and beta block thymocyte development at different stages. *Nature*, **360**, 225–231.
36. Wilson,A., Marechal,C. and MacDonald,H.R. (2001) Biased V beta usage in immature thymocytes is independent of DJ beta proximity and pT alpha pairing. *J. Immunol.*, **166**, 51–57.
37. Nativio,R., Wendt,K.S., Ito,Y., Huddleston,J.E., Uribe-Lewis,S., Woodfine,K., Krueger,C., Reik,W., Peters,J.M. and Murrell,A. (2009) Cohesin is required for higher-order chromatin conformation at the imprinted IGF2-H19 locus. *PLoS Genet.*, **5**, e1000739.
38. Ji,Y., Little,A.J., Banerjee,J.K., Hao,B., Oltz,E.M., Krangel,M.S. and Schatz,D.G. (2010) Promoters, enhancers, and transcription

target RAG1 binding during V(D)J recombination. *J. Exp. Med.*, **207**, 2809–2816.
39. Ji,Y., Resch,W., Corbett,E., Yamane,A., Casellas,R. and Schatz,D.G. (2010) The in vivo pattern of binding of RAG1 and RAG2 to antigen receptor loci. *Cell*, **141**, 419–431.
40. Volpi,S.A., Verma-Gaur,J., Hassan,R., Ju,Z., Roa,S., Chatterjee,S., Werling,U., Hou,H. Jr, Will,B., Steidl,U. *et al.* (2012) Germline deletion of Igh 3' regulatory region elements hs 5, 6, 7 (hs5-7) affects B cell-specific regulation, rearrangement, and insulation of the Igh locus. *J. Immunol.*, **188**, 2556–2566.
41. Xiang,Y., Zhou,X., Hewitt,S.L., Skok,J.A. and Garrard,W.T. (2011) A multifunctional element in the mouse Igkappa locus that specifies repertoire and Ig loci subnuclear location. *J. Immunol.*, **186**, 5356–5366.
42. Seitan,V.C., Hao,B., Tachibana-Konwalski,K., Lavagnolli,T., Mira-Bontenbal,H., Brown,K.E., Teng,G., Carroll,T., Terry,A., Horan,K. *et al.* (2011) A role for cohesin in T-cell-receptor rearrangement and thymocyte differentiation. *Nature*, **476**, 467–471.
43. Bossen,C., Mansson,R. and Murre,C. (2011) Chromatin topology and the regulation of antigen receptor assembly. *Annu. Rev. Immunol.*, **30**, 337–356.
44. Hou,C., Zhao,H., Tanimoto,K. and Dean,A. (2008) CTCF-dependent enhancer-blocking by alternative chromatin loop formation. *Proc. Natl Acad. Sci. USA*, **105**, 20398–20403.
45. Tolhuis,B., Palstra,R.J., Splinter,E., Grosveld,F. and de Laat,W. (2002) Looping and interaction between hypersensitive sites in the active beta-globin locus. *Mol. Cell*, **10**, 1453–1465.
46. Spicuglia,S., Kumar,S., Yeh,J.H., Vachez,E., Chasson,L., Gorbatch,S., Cautres,J. and Ferrier,P. (2002) Promoter activation by enhancer-dependent and -independent loading of activator and coactivator complexes. *Mol. Cell*, **10**, 1479–1487.
47. Engel,N., Raval,A.K., Thorvaldsen,J.L. and Bartolomei,S.M. (2008) Three-dimensional conformation at the H19/Igf2 locus supports a model of enhancer tracking. *Hum. Mol. Genet.*, **17**, 3021–3029.
48. Gaszner,M. and Felsenfeld,G. (2006) Insulators: exploiting transcriptional and epigenetic mechanisms. *Nat. Rev. Genet.*, **7**, 703–713.